

Published in final edited form as:

*Heart Rhythm*. 2011 December ; 8(12): 1923–1930. doi:10.1016/j.hrthm.2011.07.016.

## Subcellular heterogeneity of sodium current properties in adult cardiac ventricular myocytes

Xianming Lin, PhD<sup>1</sup>, Nian Liu, MD<sup>1</sup>, Jia Lu, PhD<sup>1</sup>, Jie Zhang, BS<sup>1</sup>, Justus Anumonwo, MB, PhD<sup>2,4</sup>, Lori L Isom, PhD<sup>3,4</sup>, Glenn I Fishman, MD<sup>1</sup>, and Mario Delmar, MD, PhD<sup>1</sup>

<sup>1</sup>The Leon H. Charney Division of Cardiology, New York University School of Medicine, New York NY

<sup>2</sup>Department of Medicine, University of Michigan, Ann Arbor MI

<sup>3</sup>Department of Pharmacology, University of Michigan, Ann Arbor MI

<sup>4</sup>Department of Molecular and Integrative Physiology, University of Michigan, Ann Arbor MI

### Abstract

**BACKGROUND**—Sodium channel  $\alpha$ -subunits in ventricular myocytes (VMs) segregate either to the intercalated disc, or to lateral membranes, where they associate with region-specific molecules.

**OBJECTIVE**—To determine the functional properties of sodium channels as a function of their location in the cell.

**METHODS**—Local sodium currents were recorded from adult rodent VMs and Purkinje cells using the cell-attached macropatch configuration. Electrodes were placed either in the cell midsection (M), or cell end (area originally occupied by the intercalated disc; ID). Channels were identified as TTX-sensitive (TTX-S) or TTX-resistant (TTX-R) by application of 100 nM TTX.

**RESULTS**—Average peak-current amplitude was larger in ID than M, and largest at site of contact between attached cells. TTX-S channels were found only in M region of VMs, and not in Purkinje myocytes. TTX-R channels were found in M and ID, but their biophysical properties differed depending on recording location. Sodium current in rat VMs was upregulated by TNF- $\alpha$ . The magnitude of current increase was largest in M, but this difference was abolished by 100 nM TTX.

**CONCLUSIONS**—Our data suggest that: a) a large fraction of TTX-R (likely Na<sub>v</sub>1.5) channels in the M region of VMs are inactivated at normal resting potential, leaving most of the burden of excitation to TTX-R channels in the ID; b) cell-cell adhesion increases functional channel density at ID. c) TTX-S (likely non-Na<sub>v</sub>1.5) channels make a minimal contribution to sodium current under control conditions, but represent a functional reserve that can be upregulated by exogenous factors.

---

© 2011 The Heart Rhythm Society. Published by Elsevier Inc. All rights reserved.

Address correspondence to: Mario Delmar, MD, PhD, The Leon H Charney Division of Cardiology, New York University School of Medicine, 522 First Avenue, Smilow805, New York NY 10016, Phone: (212)263-9492, Fax: (212)263-4129, Mario.Delmar@nyumc.org.

### CONFLICT OF INTEREST

None

**Publisher's Disclaimer:** This is a PDF file of an unedited manuscript that has been accepted for publication. As a service to our customers we are providing this early version of the manuscript. The manuscript will undergo copyediting, typesetting, and review of the resulting proof before it is published in its final citable form. Please note that during the production process errors may be discovered which could affect the content, and all legal disclaimers that apply to the journal pertain.

## Keywords

sodium current; intercalated disc; Nav1.5

## INTRODUCTION

The sodium current ( $I_{Na}$ ) plays a critical role in cardiac propagation. Previous studies describe two subpopulations of voltage-gated sodium channels (VGSCs) in ventricular myocytes: One, at the intercalated disc (ID),<sup>1-4</sup> where the tetrodotoxin-resistant (TTX-R) isoform  $Na_v1.5$  associates with beta subunits, ankyrin-G, SAP97 and junctional proteins;<sup>4-8</sup> the other, at lateral membranes where  $Na_v1.5$  associates with the syntrophin/dystrophin complex.<sup>4</sup> Whether these subpopulations represent different functional pools with distinct biophysical and regulatory properties remains undefined. Moreover, several studies show that VGSC complexes interact with molecules involved in cell-cell adhesion.<sup>8,9</sup> This interaction, likely to occur primarily at the ID, opens the possibility that preservation of cell-cell contact is relevant to VGSC function. Finally, in addition to  $Na_v1.5$ , other  $\alpha$ -subunits are present in cardiomyocytes;<sup>2,10</sup> yet, their localization, and contribution to whole-cell  $I_{Na}$ , remain unclear (e.g., Verkerk et al<sup>11</sup> vis-a-vis Petiprez and Abriel<sup>12</sup>). Here, we utilized the cell-attached, macropatch configuration<sup>11</sup> to record local  $I_{Na}$  either from the midsection (M) of a single cell, from the single cell end in the area originally occupied by the ID (single-ID), or from the site of contact between two cells (paired-ID). We show location-selective, cell adhesion-dependent differences in  $I_{Na}$  properties, with potential implications for electrical propagation in the heart.

## METHODS

Adult rat or mouse myocytes were obtained by standard methods (e.g.,<sup>7</sup>). Purkinje myocytes were dissociated from adult Cntn2-EGFP transgenic mice, as described.<sup>13</sup> All procedures were carried out in accordance with New York University guidelines for animal use and care and conformed to the *Guide for the Care and Use of Laboratory Animals* published by the US National Institutes of Health (NIH Publication 58-23, revised 1996). Experiments were conducted within 8 hours after cell isolation. Recordings were obtained in cell-attached mode. Pipette resistance was within 1.9 to 2.1 M $\Omega$ , for consistency. Details and limitations are in online supplement, and supplemental Figure I.

## RESULTS

### $I_{Na}$ properties and recording location

$I_{Na}$  differed in amplitude and kinetics depending on recording location. As shown in Figure 1A, average peak current amplitude in the M region was significantly smaller than in the ID. Furthermore, a small positive shift in steady-state activation, a negative shift in steady-state inactivation, and a slower recovery from inactivation were observed in currents from M, when compared to those from the ID (panels 1B-D; see also Table 1; data labeled “total current”). These results indicate that the magnitude and kinetics of  $I_{Na}$  vary depending on channel location.

### $I_{Na}$ and preservation of cell-cell contact

A body of work has demonstrated association between intercellular adhesion molecules, and the VGSC complexes.<sup>8,9</sup> We thus hypothesized that loss of cell-cell contact may impact  $I_{Na}$  properties. Data in Figure 2 depict  $I_{Na}$  properties recorded from the site of contact between two cells that remained attached after dissociation (“paired-ID;” data points in green); the

results are compared to those obtained from the same area, but in single myocytes (“single-ID;” data points in red; see also Online Figure I, panels B and C). Panel A shows the average peak current amplitude obtained from the two locations, demonstrating that currents were largest when cells remained in physical contact (paired-ID). No differences were observed in the voltage-dependence of steady-state activation or inactivation (panels B and C), nor in the time course of reactivation (D). Overall, the data indicate that functional VGSC density at the ID is decreased by the loss of cell-cell contact.

### **TTX-S VGSC are absent from the ID**

Sensitivity to TTX block varies among VGSC  $\alpha$ -subunits.<sup>14</sup> The most abundant  $\alpha$ -subunit in adult ventricular myocytes is a TTX-R isoform,  $\text{Na}_v1.5$ , but TTX-S isoforms are also expressed.<sup>2,10,15,16</sup> Single adult rat ventricular myocytes were exposed to 100 nM TTX, a concentration sufficient to block “brain-type” TTX-S VGSCs and yet, lower than that necessary to block  $\text{Nav}1.5$  (or  $\text{Nav}1.8$ ).<sup>16,17</sup> Cumulative data before and after TTX exposure are shown in Online Figures II and III. In the M region, block of TTX-S channels led to a decrease in average peak current amplitude (Online Figure II-A), a small shift in steady-state activation and a negative shift in steady-state inactivation (Online Figure II-B–C), consistent with the block of channels that provide a small component to the total current and that inactivate at more positive potentials.<sup>16,18</sup> In contrast, no changes in current amplitude or kinetic properties were found in recordings from the ID region (Online Figure III). Overall, these results were consistent with previous descriptions of the presence and distribution of “brain-type” TTX-S VGSCs in rat ventricular myocytes.<sup>2,10,15,16</sup> New in our findings, however, was the identification of significant differences in the properties of the TTX-R current, depending on channel location. In Figure 3, we overlay the data obtained after TTX exposure (that is, the TTX-R currents) from the M (blue points) and the ID regions (red points; examples of raw traces are shown in Online Figure IV). TTX-R current amplitude was significantly larger in the ID (Figure 3A). Steady-state activation (panel 3B) showed no region-specific differences. In contrast, steady-state inactivation in M occurred at voltages significantly more negative (panel 3C) and the recovery from inactivation in M was slower (3D) than those in the ID. As detailed in Table 1 (data labeled “TTX-R”), the average half-maximum steady-state inactivation voltage in the ID was  $-83.6 \pm 1.3$  mV, whereas in M was  $-96.5 \pm 2.3$  mV ( $p < 0.001$ ). These results lead to the prediction that the majority of VGSCs in the mid-section of an adult rat ventricular myocyte would be in the inactivated state at voltages corresponding to the cell resting potential. As shown in Online Figures V–IX, similar results were obtained from myocytes dissociated from adult mouse ventricle (quantitative data in online Table 1).

### **Region-specific differences in response to TNF- $\alpha$**

The presence of different functional VGSC pools led us to speculate that VGSC regulation may also be non-uniform. Single rat ventricular myocytes were exposed to TNF- $\alpha$ , a cytokine previously shown to be a part of the inflammatory response of the myocardium, and thought to be of potential arrhythmogenicity.<sup>19</sup> Currents were recorded from the ID or M regions. Figures 4A–C show that control peak current amplitude remained constant during ten minutes of recording (black circles). Acute addition of TNF- $\alpha$  (100 ng/ml) caused an increase in current amplitude in the M region (Figure 4A) but only a minor increase in the ID, either in single (Panel 4B), or paired cells (Panel 4C). Interestingly, in the presence of 100 nM TTX, the current increase in M (panel D) became similar to that of the ID (4B and 4C), thus suggesting that TTX-S channels in the M region of the cell are most responsive to the presence of the inflammatory cytokine.

## $I_{Na}$ in Purkinje cells

Additional experiments sought to characterize region-specific differences in  $I_{Na}$  properties recorded from murine Purkinje myocytes. As in the case of ventricular myocytes, current amplitude was larger in the ID region, when compared to the midsection of the cell (Online Figure X-A); no region-specific statistically significant differences were noted in the voltage-dependence of activation (online Figure X-B) or steady-state inactivation (online Figure X-C), or in the time course of reactivation (online Figure X-D). Two interesting differences were noted when comparing the regional properties of  $I_{Na}$  in Purkinje versus working ventricular myocytes of the same species: First, the amplitude of the current in the ID (but not in the M) region was larger in the Purkinje cells (Figure 5A–B). Second, as opposed to ventricular cells, exposure to 100 nM TTX did not affect the amplitude or the kinetics of the  $I_{Na}$  recorded from the midsection of Purkinje myocytes (Figure 6A–D). The latter result argues in favor of the notion that the expression profile of  $Na_v1.x$  subunits in Purkinje myocytes is different from that of the working ventricle.<sup>20</sup>

## DISCUSSION

Recent studies have proposed that there are two spatially-distinguishable VGSC pools in cardiomyocytes.<sup>4</sup> Functional demonstration of these channel subgroups has been lacking. Here, we confirm that  $I_{Na}$  in working ventricular myocytes includes a TTX-S component, absent from the ID, and a TTX-R component that occupies the ID. More importantly, we describe the biophysical properties of the TTX-R fraction localized to the sarcolemma. Our studies are first to demonstrate that: 1) TTX-R channels in the sarcolemma have kinetic properties different from those in the ID. 2) The magnitude of the TTX-R  $I_{Na}$  at the ID is significantly larger if cell-cell attachment is preserved, and 3) the magnitude of  $I_{Na}$  is differentially regulated by a cytokine, with current increase through TTX-S channels being proportionately larger than that through the TTX-R component. These local differences may be consequent to expression of various  $Nav1.x$  isoforms, and/or to interaction of the same  $\alpha$ -subunit, with different molecules.<sup>4–7</sup> Overall, our data suggest that: a) TTX-R (likely  $Na_v1.5$ ) channels in the M region are mostly inactivated at a normal resting potential, leaving most of the burden of excitation to TTX-R channels in the ID; b) cell-cell adhesion increases functional channel density at the ID and c) TTX-S channels have a minimum contribution to  $I_{Na}$  under control conditions, but represent a functional reserve that can be upregulated by exogenous factors. Finally, we show that a TTX-S component is not detectable (within our recording conditions) in murine Purkinje myocytes, supporting the notion of a different  $Nav1.x$  profile in the cardiac conduction system.<sup>20</sup>

### Subcellular segregation of $I_{Na}$ properties, and regional distribution of $Na_v1.5$

Our data confirm the presence of TTX-S channels in working ventricular myocytes.<sup>10,15,16</sup> Previous studies in rabbit myocytes concluded that all current from the cell mid-section was TTX-S.<sup>11</sup> The latter differs from our results in rodent cells, showing TTX-R current in the M section. Species differences may explain the results. More importantly, we discern two different functional populations of TTX-R channels: the first one present at the ID and the second one, with different inactivation and repriming kinetics, distributed along the sarcolemma. These two populations could result from expression of two different TTX-R  $Na_v1.x$  subunits. An alternative explanation is that the  $Na_v1.x$  subunit is the same, but its biophysical properties are affected by association with region-specific molecules. The first possibility seems unlikely, at least in working myocytes, where other  $Na_v$  subunits previously identified are also TTX-sensitive.<sup>14,16</sup> On the other hand, Petripez et al<sup>4</sup> concluded that  $Na_v1.5$  partners with different molecules depending on whether it localizes to the ID, or the lateral membrane. We propose that the difference in current kinetics reported here is partly consequent to these molecular associations. The latter, though speculative, is

consistent with observations demonstrating that whole-cell  $I_{Na}$  properties in myocytes lacking PKP2 expression are similar to those recorded locally in the M region (see Fig 2 in<sup>7</sup>). Further experiments will assess the dependence of Nav1.5 kinetics on non-channel molecular partners.

Based on the observed location-specific differences in kinetic properties, we speculate that the action potential upstroke of a ventricular myocyte results mostly from activation of VGSCs localized to the ID region. Given the long space constant of cardiac tissue, this subcellular segregation of functional channels would have little impact on the ability of the entire myocyte to be depolarized by VGSC activation, thus eliciting a contractile event. Furthermore, under control conditions and in a scenario where cells are highly coupled through gap junctions, these regional differences may not be very relevant to the success or failure of action potential propagation. Yet, subcellular segregation may be critical under conditions where electrical coupling is decreased.<sup>21</sup> In fact, computer simulations of action potential propagation between cardiac cells<sup>3,22</sup> suggest that the increased  $I_{Na}$  density at the ID may allow for field-mediated activation of the neighboring cell even in the absence of functional gap junctions. Further experimental and numerical studies, including accurate measurements of the volume of the intercellular gap, remain necessary to validate the latter hypothesis. Finally, it is interesting to note that experiments in mice with mutations in the dystrophin gene have revealed changes in  $I_{Na}$  properties and on conduction velocity consistent with an involvement of sarcolemmal VGSCs on action potential propagation.<sup>4</sup> We recognize that a limitation of our study is the fact that all observations have been conducted in isolated myocytes, and perhaps, channel function is different in the integrated cardiac tissue. Yet, it is also possible that disruption of the syntrophin/dystrophin complex impacts not only the function of VGSCs in the midregion of the cell but also, directly or indirectly, those channels that are distributed in the region of the ID.

### $I_{Na}$ in Purkinje myocytes

Previous studies indicate that  $I_{Na}$  in Purkinje myocytes is larger than in working cardiomyocytes.<sup>23</sup> We propose that this difference is largely consequent to increased density of functional channels at the ID. The identity of the Nav isoforms that form the functional sodium channels in Purkinje cells, and their relative contribution to the total cell current, remain unclear. Interestingly, unlike working ventricular myocytes, TTX-S currents were absent from the M region of Purkinje cells. These results are consistent not only with the presence of Nav1.5 in murine Purkinje cells,<sup>13</sup> but also with recent reports indicating the presence of *SCN10A* transcripts, which encode the TTX-R Nav1.8 sodium channel subunit.<sup>20</sup> Indeed, Nav1.8 may represent the dominant non-Nav1.5 subunit in the Purkinje myocyte and as such, a potential target for tissue-specific modification of  $I_{Na}$  in heart. Finally, it is worth noting that most of the data related to intermolecular interactions involving cardiac sodium channels have focused on Nav1.5, expressed in working myocytes.<sup>4,7,8</sup> The nature of those associations in Purkinje cells, remains unexplored.

### $I_{Na}$ regulation: Different channel pools, different functional response

Our data show that the relative increase in  $I_{Na}$  amplitude induced by TNF- $\alpha$  was largest in the M region, and this effect was blunted by 100 nM TTX. This result raises the possibility that TTX-S channels can be differentially regulated, acting as a “functional reserve” of  $I_{Na}$  upon activation of exogenous factors. It is important to note that TNF- $\alpha$  has been shown to upregulate  $I_{Na}$  in dorsal root ganglion neurons.<sup>24,25,26</sup> High levels of TNF- $\alpha$  are found in HIV patients, where this cytokine has been invoked as potentially relevant to ventricular arrhythmias.<sup>19</sup> Prolonged, systemic TNF- $\alpha$  exposure was associated with a decreased action potential upstroke velocity in murine ventricular myocytes.<sup>19</sup> To our knowledge, the acute effect of TNF- $\alpha$  on  $I_{Na}$  of ventricular myocytes has not been previously examined. Yet, it

has been described in mouse sensory neurons, and thought to result from modulation of the sodium channels by p38 mitogen-activated protein kinase, following activation of the TNF receptor TNFR1.<sup>26</sup> Whether the same mechanism applies to the effect described here, will require further studies. Upregulation of sodium channels by cytokines may be a protective mechanism to preserve fast propagation during the acute stage of inflammation.

### **I<sub>Na</sub> and intercalated disc integrity**

Cardiac Na<sub>v</sub>1.5 co-precipitates with proteins involved in intercellular communication, and cell-cell adhesion.<sup>5,7,8,27</sup> We thus proposed that I<sub>Na</sub> properties may be affected by cell-cell contact integrity.<sup>7</sup> Here, we show that when cells remain in contact, I<sub>Na</sub> is significantly larger than when cells are isolated from their neighbors. This result emphasizes the relevance of interactions between VGSCs and junctional complexes. It further suggests that I<sub>Na</sub> magnitude during propagation is larger than previously thought. Our studies invite reconsideration of numerical parameters used to describe I<sub>Na</sub> in mathematical models of cardiac electrophysiology, including those where subcellular domains are taken into account.<sup>3,21,22</sup> Finally, whether mutations in Na<sub>v</sub>1.5 or other Na<sub>v</sub> subunits, or changes in Na<sub>v</sub>1.5 abundance during acquired diseases, differentially affect one functional pool or another in a way meaningful to arrhythmia risk, remains a matter of further investigation.

### **Supplementary Material**

Refer to Web version on PubMed Central for supplementary material.

### **Acknowledgments**

#### **FUNDING**

This work was supported by National Institutes of Health HL106632, HL087226 and GM57691 to M.D., HL182727 to G.I.F., NYSYSTEM CO24327 to G.I.F., NS064245 to L.L.I and a Foundation Leducq Transatlantic Network to M.D.

### **ABBREVIATIONS**

<b>ID</b>	intercalated disc
<b>I<sub>Na</sub></b>	sodium current
<b>PKP2</b>	plakophilin 2
<b>SAP 97</b>	synapse-associated protein 97
<b>TNF-<math>\alpha</math></b>	tumor necrosis factor-alpha
<b>TTX</b>	tetrodotoxin
<b>TTX-R</b>	TTX-resistant
<b>TTX-S</b>	TTX-sensitive
<b>VGSC</b>	voltage gated sodium channel

### **References**

1. Cohen SA. Immunocytochemical localization of rH1 sodium channel in adult rat heart atria and ventricle. Presence in terminal intercalated disks. *Circulation*. 1996; 94:3083–3086. [PubMed: 8989112]

2. Maier SK, Westenbroek RE, McCormick KA, Curtis R, Scheuer T, Catterall WA. Distinct subcellular localization of different sodium channel alpha and beta subunits in single ventricular myocytes from mouse heart. *Circulation*. 2004; 109:1421–1427. [PubMed: 15007009]
3. Kucera JP, Rohr S, Rudy Y. Localization of sodium channels in intercalated disks modulates cardiac conduction. *Circ Res*. 2002; 91:1176–1182. [PubMed: 12480819]
4. Petitprez S, Zmoos AF, Ogrodnik J, et al. SAP97 and dystrophin macromolecular complexes determine two pools of cardiac sodium channels Nav1. 5 in cardiomyocytes. *Circ Res*. 2011; 108:294–304. [PubMed: 21164104]
5. Malhotra JD, Thyagarajan V, Chen C, Isom LL. Tyrosine-phosphorylated and nonphosphorylated sodium channel beta1 subunits are differentially localized in cardiac myocytes. *J Biol Chem*. 2004; 279:40748–40754. [PubMed: 15272007]
6. Lowe JS, Palygin O, Bhasin N, et al. Voltage-gated Nav channel targeting in the heart requires an ankyrin-G dependent cellular pathway. *J Cell Biol*. 2008; 180:173–186. [PubMed: 18180363]
7. Sato PY, Musa H, Coombs W, et al. Loss of plakophilin-2 expression leads to decreased sodium current and slower conduction velocity in cultured cardiac myocytes. *Circ Res*. 2009; 105:523–526. [PubMed: 19661460]
8. Sato PY, Coombs W, Lin X, et al. Interactions between ankyrin-G, plakophilin-2, and connexin43 at the cardiac intercalated disc. *Circ Res*. 2011
9. Patino GA, Isom LL. Electrophysiology and beyond: Multiple roles of Na<sup>+</sup> channel β subunits in development and disease. *Neurosci Lett*. 2010; 486:53–59. [PubMed: 20600605]
10. Dhar Malhotra J, Chen C, Rivolta I, et al. Characterization of sodium channel alpha- and beta-subunits in rat and mouse cardiac myocytes. *Circulation*. 2001; 103:1303–1310. [PubMed: 11238277]
11. Verkerk AO, van Ginneken ACG, van Veen TAB, Tan HL. Effects of heart failure on brain-type Na<sup>+</sup> channels in rabbit ventricular myocytes. *Europace*. 2007; 9:571–577. [PubMed: 17579244]
12. Petitprez S, Abriel H. Comment on: Effects of heart failure on brain-type Na<sup>+</sup> channels in rabbit ventricular myocytes. *Europace*. 2008; 10:257. author's response 2008; 10: 257–258. [PubMed: 18056137]
13. Pallante BA, Giovannone S, Liu FY, et al. Contactin-2 expression in the cardiac Purkinje fiber network. *Circ Arrhythm Electrophysiol*. 2010; 3:186–194. [PubMed: 20110552]
14. Goldin AL. Resurgence of sodium channel research. *Annu Rev Physiol*. 2001; 63:871–894. [PubMed: 11181979]
15. Maier SK, Westenbroek RE, Schenkman KA, Feigl EO, Scheuer T, Catterall WA. An unexpected role for brain-type sodium channels in coupling of cell surface depolarization to contraction in the heart. *Proc Natl Acad Sci USA*. 2002; 99:4073–4078. [PubMed: 11891345]
16. Brette F, Orchard CH. No apparent requirement for neuronal sodium channels in excitation-contraction coupling in rat ventricular myocytes. *Circ Res*. 2006; 98:667–674. [PubMed: 16484618]
17. Benn SC, Costigan M, Tate S, Fitzgerald M, Woolf CJ. Developmental expression of the TTX-resistant voltage-gated sodium channels Nav1.8 (SNS) and Nav1. 9 (SNS2) in primary sensory neurons. *J Neurosci*. 2001; 21:6077–6085. [PubMed: 11487631]
18. Kirsch GE, Brown AM. Kinetics properties of single sodium channels in rat heart and rat brain. *J Gen Physiol*. 1989; 93:85–99. [PubMed: 2536800]
19. Grandy SA, Brouillette J, Fiset C. Reduction of ventricular sodium current in a mouse model of HIV. *J Cardiovasc Electrophysiol*. 2010; 21:916–922. [PubMed: 20132381]
20. Sotoodehnia N, Isaacs A, de Bakker PI, et al. Common variants in 22 loci are associated with QRS duration and cardiac ventricular conduction. *Nat Genet*. 2010; 42:1068–1076. [PubMed: 21076409]
21. Tsumoto K, Ashihara T, Haraguchi R, Nakazawa K, Kurachi Y. Roles of subcellular Na<sup>+</sup> channel distributions in the mechanism of cardiac conduction. *Biophys J*. 2011; 100:554–563. [PubMed: 21281569]
22. Mori Y, Fishman GI, Peskin CS. Ephaptic conduction in a cardiac strand model with 3D electrodiffusion. *Proc Natl Acad Sci USA*. 2008; 105:6463–6468. [PubMed: 18434544]

23. Aslanidi OV, Sleiman RN, Boyett MR, Hancox JC, Zhang H. Ionic mechanisms for electrical heterogeneity between rabbit Purkinje fiber and ventricular cells. *Biophys J.* 2010; 98:2420–2431. [PubMed: 20513385]
24. He XH, Zang Y, Chen X, et al. TNF- $\alpha$  contributes to up-regulation of Nav1.3 and Nav1.8 in DRG neurons following motor fiber injury. *Pain.* 2010; 151:266–279. [PubMed: 20638792]
25. Chen X, Pang RP, Shen KF, et al. TNF- $\alpha$  enhances the currents of voltage gated sodium channels in uninjured dorsal root ganglion neurons following motor nerve injury. *Exp Neurol.* 2011; 227:279–286. [PubMed: 21145890]
26. Jin X, Gereau IV. Acute p38-mediated modulation of tetrodotoxin-resistant sodium channels in mouse sensory neurons by tumor necrosis factor- $\alpha$ . *J Neurosci.* 2006; 26:246–255. [PubMed: 16399694]
27. Abriel H. Cardiac sodium channel Nav1.5 and interacting proteins: Physiology and pathophysiology. *J Mol Cell Cardiol.* 2010; 48:2–11. [PubMed: 19744495]



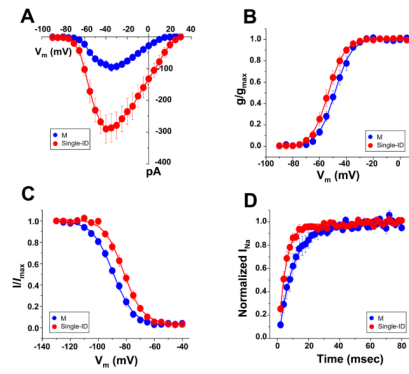


**Figure 1.** Local  $I_{Na}$  in the M (blue), and ID (single-ID; red) regions of single rat ventricular myocytes. A–D, peak current-voltage relation, steady-state activation, steady-state inactivation and reactivation, respectively. Quantitative data (including numbers of experiments in each group) in Table I.

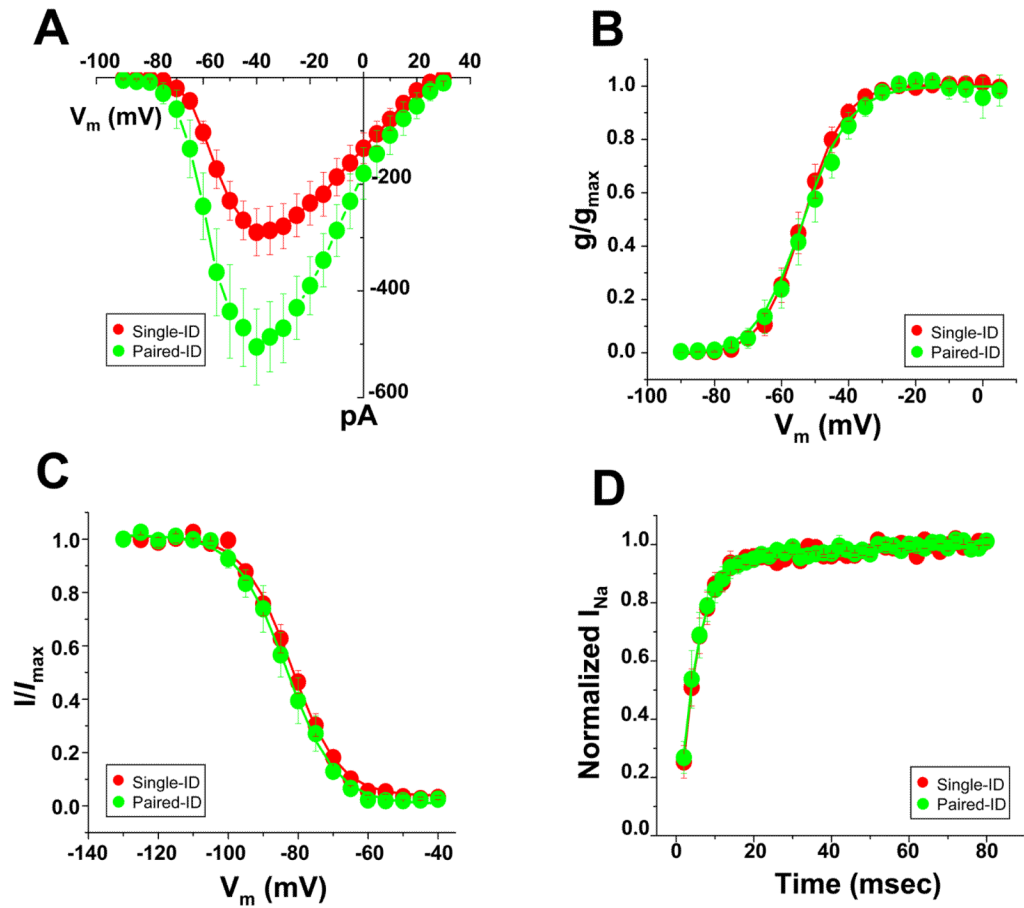


**Figure 2.** Local  $I_{Na}$  in the ID region of a single rat ventricular myocyte (“Single-ID;” red) and at the site of contact between two cells in a pair (“Paired-ID;” green). A–D, peak current-voltage relation, steady-state activation, steady-state inactivation and reactivation, respectively. Quantitative data (including numbers of experiments in each group) in Table I.

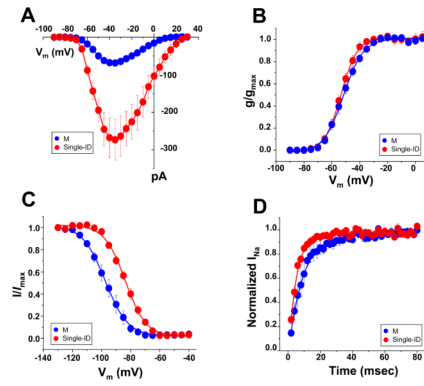


**Figure 3.** TTX-R currents in the M (blue) versus single ID (red) regions of rat ventricular myocytes. A–D: Peak current-voltage relation, steady-state activation, steady-state inactivation and reactivation, respectively. Quantitative parameters (including numbers of experiments in each group) in Table 1.

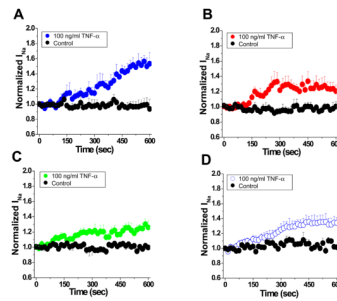


**Figure 4.**

Time course of TNF- $\alpha$  induced upregulation of sodium current recorded from M (blue; panel A), single ID (red, B) or paired-ID (green; C) ( $p < 0.05$ , M Vs single ID). Black symbols, control (no TNF- $\alpha$  added). Time zero marks addition of TNF- $\alpha$ . D: Same as A, but in 100 nM TTX ( $p < 0.05$ , compared to results obtained without TTX).

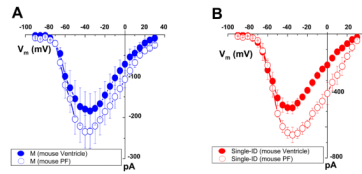


**Figure 5.** Comparison of peak current-voltage relations recorded from mouse Purkinje cells (open symbols) versus working ventricular myocytes (closed symbols). Currents were recorded from either the M (panel A) or the single-ID regions (panel B). Images of Purkinje cells dissociated from adult *Cntn2*-EGFP transgenic mice can be found in ref<sup>13</sup>. Recording sites for Purkinje cells were the same as for ventricular myocytes; see also supplemental Figure 1.

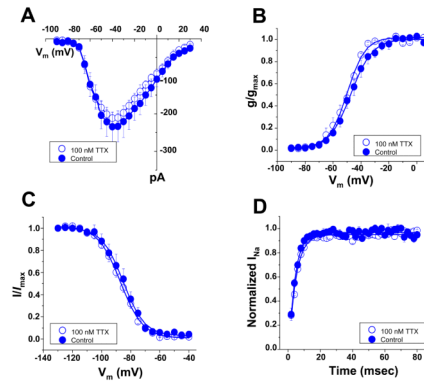


**Figure 6.** Absence of TTX-S currents in the M region of murine Purkinje cells. A–D: peak current-voltage relation, steady-state activation, steady-state inactivation and reactivation, respectively. Closed or open symbols, currents recorded in control conditions or in the presence of 100 nM TTX, respectively.

**Table 1**

Parameters of  $I_{Na}$  recorded from different locations of adult rat ventricular myocytes.

	$I_{Na, peak}$ (pA)		$V_{1/2, activation}$ (mV)		$V_{1/2, inactivation}$ (mV)		Recovery time constants (msec)	
	Total	TTX-R	Total	TTX-R	Total	TTX-R	Total	TTX-R
M	$-96.3 \pm 12.4^{\ddagger}$ (8)	$-68.8 \pm 7.3^{\ddagger}$ (8)	$-48.1 \pm 1.8^*$ (8)	$-52.9 \pm 1.5$ (8)	$-90.0 \pm 0.5^{\ddagger}$ (9)	$-96.5 \pm 2.3^{\ddagger}$ (7)	$9.3 \pm 2.4^*$ (6)	$9.6 \pm 2.0^*$ (8)
Single-ID	$-286.7 \pm 45.2$ (7)	$-273.5 \pm 53.9$ (6)	$-53.6 \pm 1.7$ (7)	$-51.7 \pm 0.3$ (6)	$-82.2 \pm 1.8$ (6)	$-83.6 \pm 1.3$ (8)	$4.8 \pm 0.8$ (7)	$4.9 \pm 0.5$ (7)
Paired-ID	$-505.2 \pm 71.2^*$ (7)	$-467.6 \pm 46.7^*$ (6)	$-53.7 \pm 2.0$ (7)	$-54.9 \pm 0.4$ (6)	$-83.7 \pm 2.5$ (6)	$-83.3 \pm 3.1$ (7)	$4.9 \pm 0.7$ (6)	$4.7 \pm 0.8$ (6)

The numbers in the parentheses indicate the number of the experiments.

M vs Single-ID,

\*  $P < 0.05$ ,

$^{\ddagger} P < 0.005$ ,

$^{\ddagger} P < 0.001$ ;

Single-ID vs Paired-ID,

\*  $P < 0.05$ .